

available at www.sciencedirect.comwww.elsevier.com/locate/brainres**BRAIN
RESEARCH****Research Report**

Visualization and quantification of NAD(H) in brain sections by a novel histo-enzymatic nitrotetrazolium blue staining technique

Irina S. Balan, Gary Fiskum, Tibor Kristian*

Department of Anesthesiology, Center for Shock, Trauma and Anesthesiology Research, University of Maryland, School of Medicine 685 W. Baltimore St., MSTF 5.34, Baltimore, MD 21201, USA

ARTICLE INFO

Article history:

Accepted 12 December 2009

Available online 28 December 2009

Keywords:

Nicotinamide adenine dinucleotide

Nitrotetrazolium blue chloride

Formazan

Histo-enzymatic

Cerebral ischemia

Cryostat brain section

ABSTRACT

A histo-enzymatic technique for visualizing and quantifying endogenous NAD(H) in brain tissue was developed, based on coupled enzymatic cycling reactions that reduce nitrotetrazolium blue chloride to produce formazan. Conditions were used where the endogenous level of nicotinamide adenine dinucleotides (NAD(H)) was the rate limiting factor for formazan production. Spontaneous degradation of NAD⁺ that occurs during incubation of thawed tissue was minimized by the addition of nicotinamide mononucleotide, an inhibitor of NAD⁺ glycohydrolases. Cryostat sections of brains obtained from rats immediately after decapitation and 30 min later were used to determine the effects of ischemia alone on brain NAD(H) levels and neuroanatomic distribution. The ischemic insult resulted in a greater than 50% decline in the rate of formazan generation in the CA1 pyramidal neuronal layer of the hippocampus and in the parietal cortex and striatum, but not in the CA3 and dentate gyrus (DG) subregions of the hippocampus. The ischemia-induced changes in NAD(H) levels were confirmed by utilizing spectrofluorimetric measurements of NAD(H) present in perchloric acid extracts of brain samples. This new histo-enzymatic technique is suitable for visualizing and quantifying relative NAD(H) levels in the brain. This assay could prove useful in identifying region-selective NAD(H) catabolism that may contribute to neurodegeneration.

© 2009 Elsevier B.V. All rights reserved.

1. Introduction

NAD(H) plays critical roles in cell energy metabolism, calcium homeostasis, aging and death. It affects cell survival by various mechanisms including controlling cellular bioenergetics, mitochondrial permeability transition pore opening, and apoptosis-

inducing factor (Di Lisa et al., 2001; Ying, 2006, 2007, 2008a, 2008b; Ying et al., 2007; Liu et al., 2009; Xia et al., 2009). Since energy failure, mitochondrial calcium dysregulation and cell death are the key components in the tissue-damaging cascade initiated by cerebral or myocardial ischemia, it is likely that NAD(H) plays a significant role in ischemic brain and heart injury. NAD(H) levels

* Corresponding author.

E-mail address: tkristian@anes.umm.edu (T. Kristian).

Abbreviations: 3-AB, 3-aminobenzamide; Abs, optical absorbance; cADPR, cyclic ADP-ribose; DG, dentate gyrus; Nam, nicotinamide; NAD⁺, NADH, NAD(H), nicotinamide adenine dinucleotides; NBT, nitrotetrazolium blue chloride; NMN, nicotinamide mononucleotide; NMNAT, nicotinamide mononucleotide adenylyltransferase; PARP, poly ADP-ribose polymerase; PCA, perchloric acid

in ischemic tissue can fall, due to permeation through leaky membranes, by inhibition of *de novo* NAD⁺ synthesis or the NAD⁺ salvage pathway, and by enzymatic degradation through activation of NAD⁺ glycohydrolases (Klein et al., 1981b; Schaper and Schaper, 1983; Snell et al., 1984).

Incubation of heart or brain sections with tetrazolium salts is used as a technique to visualize the damaged regions of post-ischemic tissue and to evaluate the size of the infarcted area. This technique depends upon redox enzyme activities and cofactors present in cells that are capable of reducing the colorless, soluble tetrazolium salt to the intensely dark-colored formazan (Klein et al. 1981a; Schaper and Schaper, 1983; Liszczak et al., 1984; Bederson et al., 1986; Ridenour et al., 1992). The tetrazolium salt is reduced to formazan by diaphorases in the presence of NADH that serves as the electron donor (Klein et al., 1981a). Conversely, the non-stained tissue is considered dead due to the lack of enzymatic activity resulting from either lack of substrate, hydrolysis of cofactors (NAD(H)), or direct inactivation of enzymes, e.g., by proteolysis. Some authors have also suggested that decreased NADH-producing dehydrogenase enzyme activities play a key role (Nachlas and Shnitka, 1963) whereas others (Klein et al. 1981a, 1981b) argue that the loss of cofactors and substrates following short-term ischemia is responsible for differences in the staining. Moreover, Schaper and Schaper (1983) observed that the decreased tissue content of NAD⁺ after myocardial ischemia, rather than reduced dehydrogenase enzyme activities, was the basis for histo-enzymatic reactions employing tetrazolium salts. One of the important limitations of the current tetrazolium-based techniques is that they are often used on gross tissue slices (Bederson et al., 1986; Khalil et al., 2006) that do not allow visualization of micro-anatomic changes within the affected tissue.

The primary aim of the present study was to modify and improve the tetrazolium staining technique allowing identification of relative NAD(H) levels in different brain sub-regions and cell types. The secondary aim was to determine if this histo-enzymatic method can be used to quantify changes in brain NAD(H) after global cerebral ischemia. Our data indicate that the slower formazan accumulation rates in ischemic brain tissue are due to lower NAD(H) levels. To prevent NAD⁺ hydrolysis in brain tissue slices during the staining procedure, we added the NAD⁺ glycohydrolase inhibitor, nicotinamide mononucleotide (NMN), to the assay incubation medium. Our NAD(H) histo-enzymatic technique enables identification of microscopic (intracellular) changes in brain tissue NAD(H) content following global cerebral ischemia that was not previously possible and should therefore be applicable to many experimental paradigms where cell-selective NAD(H) catabolism may be important.

2. Results

2.1. NAD(H)-dependent enzymatic generation of formazan in tissue sections

We modified the tetrazolium staining technique to allow its use as a tool to visualize and estimate relative NAD(H) levels in tissue sections. The schematic diagram of the cyclic enzy-

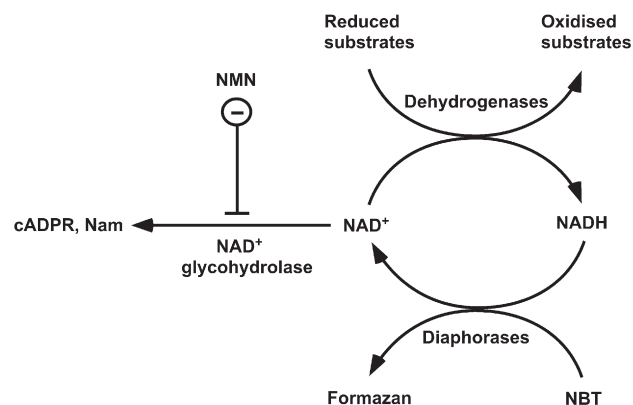


Fig. 1 – Diagram illustrating the enzymatic cycling reactions of the NAD(H)-dependent formazan generation in tissue sections. NBT is reduced to dark-colored water-insoluble formazan by tissue diaphorases in the presence of NADH, which is oxidized to NAD⁺. In turn, NAD⁺ is reduced back to NADH by various dehydrogenases in the presence of their oxidizable substrates. NAD⁺ can be degraded in the tissue by NAD⁺ glycohydrolases. This is inhibited by NMN that prevents NAD⁺ hydrolysis to cyclic ADP-ribose (cADPR) and nicotinamide (Nam). Since our assay medium contains excess of substrate for dehydrogenases the limiting factor for the rate of formazan production is the tissue NAD(H) level.

matic assay that converts tetrazolium salt to formazan in tissue is shown in Fig. 1. Our assay medium contained oxidizable substrates (malate and glutamate) for tissue dehydrogenases that reduce NAD⁺ to NADH. In the presence of NADH, diaphorases convert nitrotetrazolium blue chloride (NBT) to the darker-colored formazan. Prior to histo-enzymatic measurements, we utilized spectrofluorometric measurements of NAD(H) in homogenates of brain tissue slices after they had been incubated at different times to determine if measures were needed to inhibit possible spontaneous NAD(H) degradation that might occur during tissue incubation. As Fig. 2 shows, after 2 min of incubation, 85 % of the NAD(H) was hydrolyzed and after 5 min, the NAD(H) was almost completely degraded. This rapid and extensive NAD(H) degradation was prevented when the incubation medium contained

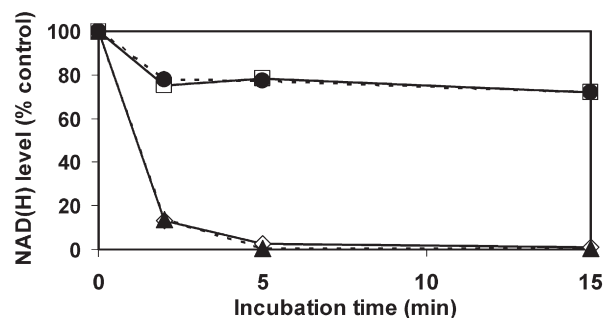


Fig. 2 – Rapid endogenous NAD(H) degradation in homogenates from control rat forebrains during incubation at 37 °C. Incubation medium consisted of 100 mM Tris-base buffer, 5 mM malate, 5 mM glutamate (◇), plus 5 mM NMN (□), plus 1 mM 3-AB (▲), or plus 1 mM AMP and 5 mM NMN (●).

5 mM nicotinamide mononucleotide (NMN), suggesting that tissue NAD⁺ glycohydrolase activities were responsible for NAD⁺ catabolism. Another enzyme known to degrade NAD⁺ is poly ADP-ribose polymerase (PARP); however, 3-aminobenzamide (3-AB), a PARP inhibitor, had no effect on the decline in NAD(H) levels observed during tissue incubation. Since NMN is a precursor for NAD⁺, the NAD(H) content could be maintained by generation via the salvage pathway using NMN adenyltransferase (NMNAT) activity (Magni et al., 2004). This reaction requires ATP. Since ATP is rapidly hydrolyzed when frozen tissue is thawed and since NMNAT is inhibited by AMP, which accumulates during ATP degradation, it is unlikely that NMN preserves NAD(H) levels by serving as a substrate for the salvage pathway. Nevertheless, we examined this possibility by adding AMP together with NMN to the incubation media. As Fig. 2 shows, the presence of AMP did not alter the NAD(H) levels, suggesting that the NAD generation was not supported by NMN and supporting the interpretation that NMN inhibits NAD(H) degradation.

Formazan accumulation rates of the cyclic enzymatic reactions described in Fig. 1 can be affected by alterations in NAD(H) concentration and also by changes in the activities of tissue dehydrogenases and diaphorases. To confirm that formazan generation was limited by endogenous levels of NAD(H), tissue from normal and ischemic brains were incubated with the histo-enzymatic assay medium containing different concentrations of exogenous NAD⁺ of from 1 to 1000 μ M. While rates were lower for ischemic tissue at 1 μ M exogenous NAD⁺, rates for both normal and ischemic tissue were saturated and very similar at 20, 100 and 1000 μ M NAD⁺ (Fig. 3). Thus, any potential differences in tissue NAD⁺ dehydrogenase activities were not responsible for differences in rates of formazan production between normal and ischemic

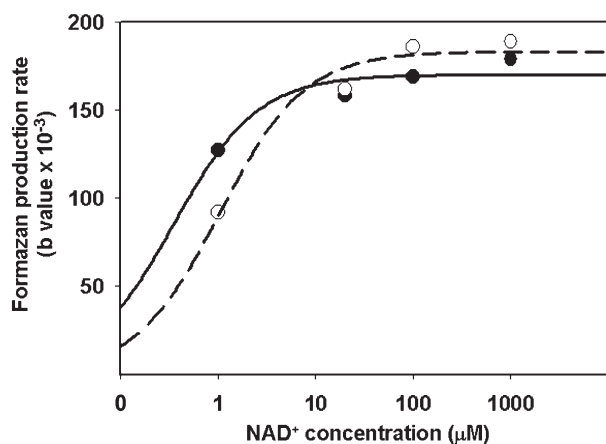


Fig. 3 – NAD⁺ concentration dependent production of formazan in the CA1 hippocampal area of rat brain tissue slices. Tissue slices prepared from frozen control (solid line) and 30 min ischemic (dash line) rat forebrains were incubated with the histo-enzymatic assay medium containing different concentrations of exogenous NAD⁺ (from 1 to 1000 μ M). For each NAD⁺ concentration the sections were incubated with assay medium for 14 different time periods (from 10 s to 30 min) and the rate of formazan production was determined.

tissues. Similarly, no differences were observed in formazan production in the presence of exogenous 1 mM NADH (not shown), indicating that any possible differences in diaphorase activities were not responsible for differences in formazan generation between normal and ischemic tissue.

2.2. Histo-enzymatic visualization of NAD(H) in brain sections

Fig. 4A provides typical examples of NAD(H) histo-enzymatic staining (accumulation of formazan) in selected brain regions following different periods during which freshly thawed tissue was incubated in the reaction media. Formazan accumulated preferentially in the pyramidal cell layer of the hippocampus. Although the staining appeared relatively uniform in the hippocampal pyramidal layer following 2–3 min incubation, longer incubation periods (6 min or more) resulted in darker staining also in the stratum radiatum and stratum oriens. Similarly, there was clear staining particularly of the perinuclear regions and proximal processes of cortical neurons after a 6-min incubation period (Fig. 4B). This staining was heterogeneous, however, characterized by different levels of dark precipitates present in individual sub-populations of neurons. Since most of the cellular NAD(H) is localized in mitochondria (Mayevsky and Rogatsky 2007), the punctuate appearance of intracellular precipitates suggests intraorganellar (presumably mitochondrial) localization of NAD(H). Therefore, the mitochondrial NAD(H) pool is probably the major contributor to tissue formazan generation. Short incubation times (20–60 s) resulted in selective staining of a subpopulation of neurons in sections from the striatum, with formazan accumulation most pronounced in perinuclear areas (Fig. 4C). Six min incubation resulted in relatively uniform staining of the whole tissue with less-stained (brighter) patches representing the cross-sections of axonal bundles (Fig. 4C). The pattern of staining in tissue sections from ischemic brains was similar to that of control brains; however, the staining intensity was much weaker at the corresponding shorter incubation periods (Figs. 4A–C). When the tissue sections were incubated for 10 min or longer, the difference in staining intensity between the control and ischemic brains became less obvious.

Fig. 5 provides quantification of changes in formazan-based optical absorbance within brain tissues, using Meta-Morph software. The data were fitted using an equation describing exponential growth to maximum with three parameters (see Experimental procedures). The values of the parameter related to formazan accumulation rates represent the relative levels of NAD(H) present in the tissues. In all structures following 15 min incubation, the staining of sections from both control and ischemic brains was saturated. The effect of the presence of the NAD⁺ glycohydrolase inhibitor NMN on rates of formazan production is shown in Figs. 6A, B. As expected, NMN significantly increased the rate of formazan generation in most of the structures examined in sections from both control and ischemic brains. Staining in the CA3 sector of the hippocampus was not significantly affected by NMN; however, there was a tendency towards a faster accumulation rate. The comparison of formazan production rates in the presence of NMN within tissue slices

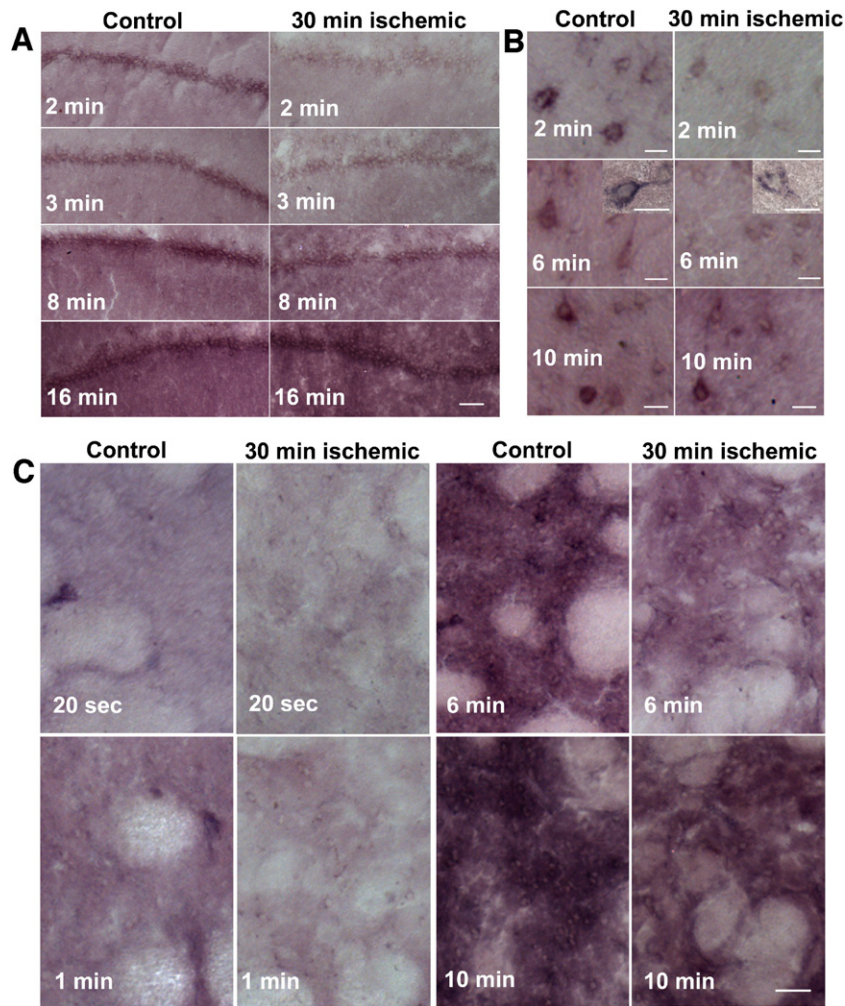


Fig. 4 – Formazan formation in (A) the CA1 sector of the hippocampus; (B) cortex, and (C) striatum of control and 30 min ischemic post-decapitated rat brains following different time periods of incubation with the histo-enzymatic assay medium. Bar sizes are (A) 100 μm ; (B) 30 μm ; (C) 75 μm .

from control and ischemic tissue is shown in Fig. 7A. The ischemic insult clearly resulted in a much slower formazan production in the CA1 sector of the hippocampus, striatum and also in cortex. Interestingly, there was no difference in the CA3 and the DG sub-regions of the hippocampus between control and ischemic tissue. To confirm that our histo-enzymatic staining correlates with changes in tissue NAD(H) levels, we dissected the desired brain areas and determined the NAD(H) content in homogenates of these samples by spectrofluorimetry. As Fig. 7B shows, ischemia caused a significant decrease in NAD(H) content in the hippocampal CA1 sector, striatum and cortex, but no significant change in NAD(H) levels in CA3 and DG. These data confirm that our histo-enzymatic staining assay can be used to assess the changes in relative levels of tissue NAD(H).

3. Discussion

The ability of non-injured cells to reduce tetrazolium salt to colored formazan was utilized as a new approach to visualize

and quantify metabolic alterations in frozen brain tissue sections obtained following an ischemic insult. The conversion of tetrazolium salt to formazan depends on coupled enzymatic cycling reactions where the tetrazolium salt is reduced to formazan by tissue diaphorases in the presence of NADH as cofactor. NADH is oxidized during this process to NAD^+ . To continue formazan generation, NAD^+ must be continually reduced back to NADH by dehydrogenases, utilizing the reducing power of various dehydrogenase substrates, e.g., malate, glutamate, etc. The rate at which formazan accumulates can therefore be dependent on a number of factors, including the activity of tissue dehydrogenases and diaphorases, dehydrogenase substrates, and the amount of NAD(H) present in the tissue.

Changes in tetrazolium-dependent staining of damaged tissue have been reported, without a consistent explanation. Nachlas and Shnitka (1963) suggested that a reduction in staining of infarcted heart tissue is lacking dehydrogenase activity therefore remains unstained. Other investigators have argued that the decrease in pyridine nucleotides and substrates in ischemic tissue, rather than reduction of dehydrogenase

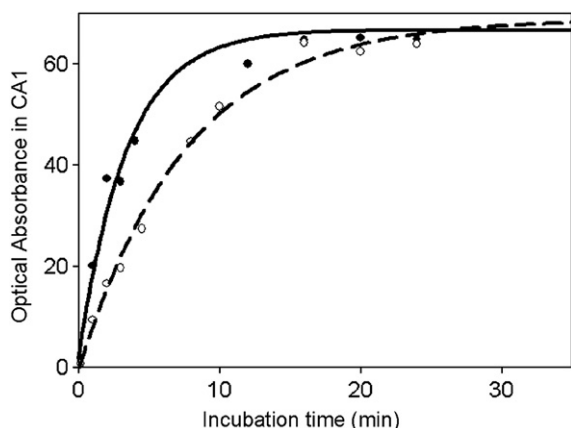


Fig. 5 – Typical example of formazan accumulation-dependent increase in optical absorbance in the CA1 sector of the hippocampus. Control tissue (solid line) and 30 min ischemic tissue (dash line) following different time periods of incubation with the assay medium. Data are fitted with SigmaPlot software using equation describing exponential growth to maximum with three parameters.

activity affects tetrazolium driven histo-enzymatic reactions (Klein et al. 1981a, 1981b; Schaper and Schaper, 1983). These early, non-quantitative approaches did not control for spontaneous NAD(H) degradation or for dehydrogenase substrate availability, as accomplished by our experiments. The results of these measurements conclusively demonstrate that there is region-selective reduction in formazan staining in the rat brain after ischemia, due to a loss of NAD(H).

NAD(H) plays an extremely important role in many oxidation-reduction reactions present in central pathways of energy metabolism, e.g., glycolysis, the TCA cycle, and oxidative phosphorylation. These reactions catalyze interconversion between the oxidized and reduced forms of NAD(H). NAD⁺ also serves as a substrate for enzymes that do not simply reduce it to NADH but that catalyze reactions with the potential to deplete the total pool of NAD(H). Examples include PARPs, sirtuins, and glycohydrolases. PARP is activated by oxidative stress and has been strongly implicated in the catabolism of NAD(H) that occurs during reperfusion following cerebral ischemia (Endres et al., 1997; Ying, 2008a). Furthermore, cytosolic NAD(H) levels can be modulated by activity of cyclic ADP-ribose synthases (Belenky et al., 2007). A rapid degradation of endogenous NAD⁺ was observed in canine heart homogenates (Nunez et al., 1976) and a fast exogenous NAD catabolism was detected in rat brain synaptosome extracts (Snell et al., 1984).

Tissue FADH₂ and NADPH can also serve as electron donors and cause conversion of NBT to formazan. However, their contribution is almost negligible relative to NAD(H). This is supported by our data (Fig. 6) showing that inhibition of tissue NAD(H) degradation by NMN significantly increased formazan production rates both in non-ischemic and ischemic tissues (Figs. 6A, B).

In light of the potential for rapid catabolism of NAD(H) during 37 °C thawing and incubation of frozen brain tissue, experiments were performed in the absence and presence of

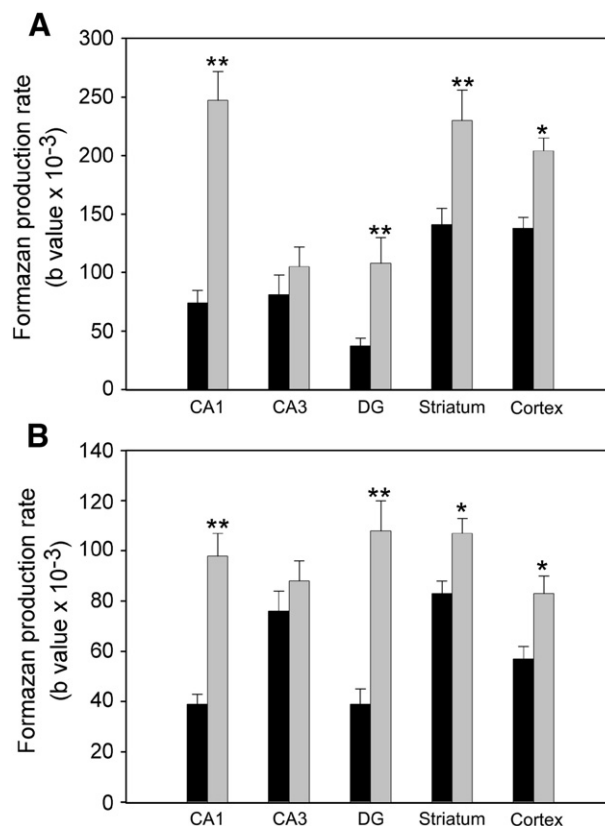


Fig. 6 – Effect of NMN on tissue NAD(H) degradation. (A) control brain tissue. (B) 30 min ischemic brain tissue. The NMN significantly inhibited the NAD(H) depletion in both control and ischemic samples. Black bars represent the data when the reaction mixture does not contain NMN, and gray bars represent the data when 5 mM NMN is added in the mixture. Interestingly, in the CA3 region of the hippocampus there was no significant effect of the NMN on NAD⁺ catabolism. The sections were incubated with the corresponding assay medium for 14 different time periods (from 10 s to 30 min), n=4; *P<0.01; **P<0.001.

inhibitors of different NAD⁺ catabolizing enzymes. In the absence of these inhibitors, tissue NAD(H) was almost completely degraded after 5 min incubation (Fig. 2). The presence of the PARP inhibitor 3-AB had no effect on NAD(H) catabolism whereas about 80 % of tissue NAD(H) was still present after 5 min incubation in the presence of the NAD⁺ glycohydrolase inhibitor NMN (Okayama et al., 1980; Snell et al., 1984). The finding that AMP, an inhibitor of potential NAD(H) biosynthesis from NMN, had no effect on tissue levels of NAD(H) indicates that NMN preserved tissue NAD(H) through inhibition of catabolism rather than stimulation of NAD(H) production.

Since variability in the activities of tissue dehydrogenases and the diaphorases can also affect formazan production under the conditions used in our histo-enzymatic assay, it was necessary to perform experiments to exclude such variability as a cause for different results obtained with normal and ischemic brain tissue. The finding shown in Fig. 3 that maximal rates of formazan production in the presence of

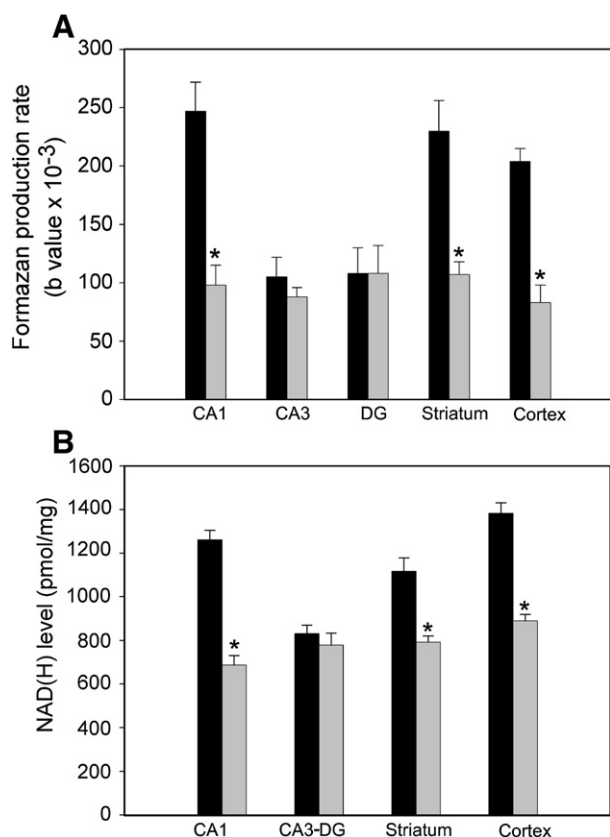


Fig. 7 – Comparisons of (A) formazan accumulation rates and (B) NAD(H) contents after PCA extraction in the CA1, CA3, DG, striatum and cortex between 30 min ischemic (gray bars) and control (black bars) tissue. $n=4$; $*P<0.001$.

saturation exogenous NAD^+ were the same for both control and ischemic tissue indicates that possible differences in dehydrogenase activities were not responsible for differences observed in the absence of exogenous NAD^+ . Possible differences in diaphorase activities were similarly excluded as responsible based on the equal rate of formazan production observed with the two types of tissue in the presence of exogenous $NADH$.

Our $NAD(H)$ -dependent histo-enzymatic staining of control and ischemic brains revealed that the formazan accumulated in the hippocampus preferentially in the neuronal pyramidal layer suggesting higher $NAD(H)$ levels in cell somatic areas when compared to processes. Staining within neurons was also more pronounced in the cortex and striatum, particularly in the perinuclear regions and proximal processes. Staining within non-neuronal cells became evident at longer incubation times, but was particularly low at all times in white matter compared to grey matter. The pattern of staining in tissue sections from ischemic brains was similar to control brain sections; however, the staining intensity in the ischemic tissue was much weaker at short incubation periods. In all structures following 10- to 15-min incubation, both control and ischemic sections showed saturation of staining. However, as mentioned above, the formazan accumulation can be affected not only by $NAD(H)$ levels but also by changes in diaphorase and dehydrogenase enzyme activity. Thus, higher

rates of staining infer higher $NAD(H)$ levels only when the enzymes activities are not altered.

Our NBT histo-enzymatic technique revealed a quantitatively significant decrease in $NAD(H)$ levels present in the CA1 area of the hippocampus, the cortex, and the striatum following 30 min decapitation ischemia. In contrast, the $NAD(H)$ levels present in the CA3 and the DG sub-regions of the hippocampus were not significantly altered by the ischemic insult. The ischemia-induced changes assessed with NBT histo-enzymatic staining reflect decrease in $NAD(H)$ levels only when the activity of enzymes participating in formazan generation are not inhibited (as shown in Fig. 3). Nevertheless, the spectrofluorimetric measurement of $NAD(H)$ present in PCA extracts of the corresponding dissected brain regions of ischemic and control animals confirmed these results.

We conclude that our modified NBT histo-enzymatic technique is a suitable assay to determine relative $NAD(H)$ levels in different brain regions and to visualize $NAD(H)$ levels at microscopic levels.

4. Experimental procedures

4.1. Materials

NBT (N6876), NMN (N3501), NAD (N8285), $NADH$ (N4505), AMP (A2252), 3-AB (A0788), Malic acid (M-6413), Tris (T-8524), Resazurin (R7017), Alcohol Dehydrogenase (A-3263), Diaphorase (D-5540) were obtained from Sigma Chemical. Glutamic acid (A125-100) was obtained from Fisher Scientific.

4.2. Histo-enzymatic assay for visualizing and estimating $NAD(H)$ levels in brain sections

Brains of adult male Fisher 344 rats (300–400 g; Charles River Laboratories, Wilmington, MA) were fresh frozen immediately (control brains) or 30 min after decapitation (ischemic brains) by placing in a mold with Tissue-Tek/OCT and immersing the mold in $-30\text{ }^{\circ}\text{C}$ isopropanol cooled in liquid nitrogen. Since it took about 30 s to remove the brain from the skull and freeze it, the control brains were subjected to a very short 30-s period of ischemia. Animal experiments were performed in accordance with the Guide for the Care and Use of Laboratory Animals and approved by the University of Maryland Institutional Animal Care and Use Committee. Thirty μm frontal brain sections were generated with a cryostat and collected onto cold, clean glass slides prepared with Vectabond medium (Vector Labs, SP-1800). We collected the coronal sections from the rostrocaudal direction that contained the middle part of striatum and the middle part of hippocampus. Each glass slide contained one section from the control brain and one from ischemic brain (approximately at the same rostrocaudal level) and was stored at $-80\text{ }^{\circ}\text{C}$.

The assay medium, prepared fresh on the day when the histo-enzymatic assay was performed, consisted of 100 mM Tris-base, 5 mM malic acid, 5 mM glutamic acid, 5 mM NMN, and 1mg/ml NBT (pH 8.5). Alkaline pH was necessary to avoid spontaneous precipitation of NBT. Ten mg/ml NBT stock solution was freshly prepared in distilled water. Stock solutions of malic acid (0.5 M) and glutamic acid (0.5 M) were

prepared with Tris-base buffer and kept at -20°C . 500 mM stock solution of NMN in water was also stored at -20°C .

Slides were removed from the -80° freezer and placed immediately on dry ice. The histo-enzymatic reaction was started by adding 500 μl of the assay medium onto the glass slides immediately after removing them from the dry ice and placing them onto a 37°C slide heating stage. The slides were covered with a Hybrislip Hybridization coverslip (Invitrogen, H18202) and incubated with the assay medium in the dark at 37°C for different times of from 10 s to 30 min. The reaction was stopped by rinsing the slides three times in distilled water for 3 min. Then, the sections were dried in room air overnight in the dark and then coverslipped with VectaMount mounting medium (Vector Labs, T0116). Using the MetaMorph program, we measured changes in optical absorbance due to formazan production in pyramidal layers of three different sub-regions of the hippocampus (CA1, CA3, and DG), in three layers (from layer 4 to layer 6) of overlying parietal cortical areas, and in the striatum, excluding fiber bundles. Light microscopic $10\times$ magnification images of the desired areas of control and ischemic brains were taken at the same time using NeuroLucida software in 8 bit gray scale. Then, using the MetaMorph program, we measured average intensities of the outlined brain areas that correspond to intensity amplitudes of all pixels in the object divided by area. The absorbance of each outlined brain area was calculated by subtracting the measured intensity amplitude (I) from maximum pixel intensity amplitude (I_{max}) in brain slice images.

$$\text{Absorbance} = I_{\text{max}} - I$$

$I_{\text{max}} = 255$ (pixel values are from 0 to 255);

I = measured pixel intensity amplitude.

To quantify the background absorbance we additionally incubated some sections with the reaction mixture not containing NBT and determine the average absorbance values of the regions of interest. These were subtracted from the absorbance values determined at incubation with standard assay containing NBT. Since formazan dye is insoluble in water, it precipitates at the sites where the enzymatic reaction occurred. The sections were analyzed the next day after being mounted and cover-slipped. To avoid variability, it was critical to keep the sections in the dark from the beginning of the reaction until the generation of NeuroLucida images.

4.3. Determination of the NAD(H)-dependent formazan production in brain tissue slides

In our assay NAD^+ is reduced by dehydrogenases to NADH that is used by diaphorases to reduce the tetrazolium salt to formazan (Fig. 1). This coupled cyclic system drives formazan generation, which is dependent on NAD(H) levels but is independent of the NAD(H) redox state. The formazan accumulation over time can be described using the following equation that characterizes the exponential rise to maximum (Valero et al., 1995; Valero and Garcia-Carmona, 1996):

$$\text{Abs} = a(1 - e^{-bt}) + d;$$

where Abs is the average absorbance reflecting the amount of formazan production, a is the maximal absorbance, b is a

parameter characterizing formazan accumulation rate in tissue, t is incubation time with the assay medium, and d is the background absorbance. Data fitting was performed with the SigmaPlot Scientific Graphing System using the above-described formula. The SigmaPlot regression software calculated the value of the b parameter that represents the formazan accumulation rate.

To prevent NAD^+ degradation during the incubation of slices with the assay medium at 37°C , we used 5 mM NMN, an NAD glycohydrolase inhibitor (Okayama et al., 1980; Snell et al., 1984).

4.4. Measurement of NAD(H) levels in brain tissue

NAD(H) content in the tissue of different brain regions was determined following PCA extraction using a cyclic enzymatic assay (Richards et al., 2006). After decapitation, the brains were immediately removed from the skull and transferred into ice-cold saline. Then four different brain regions were rapidly dissected on ice and frozen in liquid nitrogen. These regions included two from the hippocampus (CA1, CA3+DG (Elmer et al. 1998), the parietal cortex (at the level of the dorsal hippocampus), and the striatum. The frozen tissue (stored at -80°C) was homogenized with 7% PCA and centrifuged as previously described (Klingenberg, 1985). In neutralized PCA extracts (10 μl), NAD(H) was determined fluorimetrically using a cycling assay medium consisting of 60 μM ethanol, 2 U alcohol dehydrogenase, 0.3 U diaphorase, 2 μM resazurin, in 0.1 M Tris and 0.1 mM EGTA buffer (pH 7.0). The sample measurement was calibrated by adding a 100 pmol of NAD^+ .

4.5. NAD(H) catabolism

Free-floating 30 μm rat brain cryostat sections were incubated in 100 mM Tris-base containing 5 mM malate and 5 mM glutamate (pH 8.5) at 37°C for 2, 5, and 15 min. The NAD(H) present in 7% PCA extracts obtained at these incubation times was measured spectrofluorimetrically, as described above. To identify the NAD^+ catabolizing enzyme, we incubated the brain tissue sections in the presence of the following inhibitors: 1 mM 3-AB (PARP inhibitor) or 5 mM NMN (NAD^+ glycohydrolase inhibitor). To exclude the possible involvement of exogenous NMN in NAD^+ synthesis in the brain tissue, we also added 1 mM AMP to the NMN solution to inhibit endogenous NMNAT activity that converts NMN to NAD^+ .

4.6. Statistical analysis

Values are means \pm Std. Error. Comparisons were performed using two-way analysis of variance (ANOVA) followed by the Student–Newman–Keuls test. Differences were considered significant at $P \leq 0.05$.

Acknowledgments

This work was supported by NIH R01 NS34152 and P01 HD16596 to G.F., R21 NS058556 to T.K., and T32 GM075776 to I.B.

REFERENCES

- Bederson, J.B., Pitts, L.H., Germano, S.M., Nishimura, M.C., Davis, R.L., Bartkowski, H.M., 1986. Evaluation of 2,3,5-triphenyltetrazolium chloride as a stain for detection and quantification of experimental cerebral infarction in rats. *Stroke* 17, 1304–1308.
- Belenky, P., Bogan, K.L., Brenner, C., 2007. NAD⁺ metabolism in health and disease. *Trends Biochem. Sci.* 32, 12–19.
- Di Lisa, F., Menabo, R., Canton, M., Barile, M., Bernardi, P., 2001. Opening of the mitochondrial permeability transition pore causes depletion of mitochondrial and cytosolic NAD⁺ and is a causative event in the death of myocytes in postischemic reperfusion of the heart. *J. Biol. Chem.* 276, 2571–2575.
- Elmer, E., Kokaia, Z., Kokaia, M., Carnahan, J., Nawa, H., Lindvall, O., 1998. Dynamic changes of brain-derived neurotrophic factor protein levels in the rat forebrain after single and recurring kindling-induced seizures. *Neuroscience* 83, 351–362.
- Endres, M., Wang, Z.Q., Namura, S., Waeber, C., Moskowitz, M.A., 1997. Ischemic brain injury is mediated by the activation of poly(ADP-ribose)polymerase. *J. Cereb. Blood Flow Metab.* 17, 1143–1151.
- Khalil, P.N., Siebeck, M., Huss, R., Pollhammer, M., Khalil, M.N., Neuhof, C., Fritz, H., 2006. Histochemical assessment of early myocardial infarction using 2,3,5-triphenyltetrazolium chloride in blood-perfused porcine hearts. *J. Pharmacol. Toxicol. Methods* 54, 307–312.
- Klein, H.H., Puschmann, S., Schaper, J., Schaper, W., 1981a. The mechanism of the tetrazolium reaction in identifying experimental myocardial infarction. *Virchows Arch.* 393, 287–297.
- Klein, H.H., Schaper, J., Puschmann, S., Nienaber, C., Kreuzer, H., Schaper, W., 1981b. Loss of canine myocardial nicotinamide adenine dinucleotides determines the transition from reversible to irreversible ischemic damage of myocardial cells. *Basic Res. Cardiol.* 76, 612–621.
- Klingenberg, M., 1985. Nicotinamide-adenine dinucleotides spectrophotometric and fluometric methods. In: Bergmeyer, H.U. (Ed.), *Methods in Enzymatic analysis*. Verlag Chemie, Weinheim, pp. 2045–2072.
- Liszczyk, T.M., Hedley-Whyte, E.T., Adams, J.F., Han, D.H., Kolluri, V.S., Vacanti, F.X., Heros, R.C., Zervas, N.T., 1984. Limitations of tetrazolium salts in delineating infarcted brain. *Acta Neuropathol.* 65, 150–157.
- Liu, D., Gharavi, R., Pitta, M., Gleichmann, M., Mattson, M.P., 2009. Nicotinamide prevents NAD⁺ depletion and protects neurons against excitotoxicity and cerebral ischemia: NAD⁺ consumption by SIRT1 may endanger energetically compromised neurons. *Neuromolecular Med.* 11, 28–42.
- Magni, G., Amici, A., Emanuelli, M., Orsomando, G., Raffaelli, N., Ruggieri, S., 2004. Enzymology of NAD⁺ homeostasis in man. *Cell. Mol. Life Sci.* 61, 19–34.
- Mayevsky, A., Rogatsky, G.G., 2007. Mitochondrial function in vivo evaluated by NADH fluorescence: from animal models to human studies. *Am. J. Physiol. Cell Physiol.* 292, 615–640.
- Nachlas, M.M., Shnitka, T.K., 1963. Macroscopic identification of early myocardial infarcts by alterations in dehydrogenase activity. *Am. J. Pathol.* 42, 379–405.
- Nunez, R., Calva, E., Marsch, M., Briones, E., Lopez-Soriano, F., 1976. NAD glycohydrolase activity in hearts with acute experimental infarction. *Am. J. Physiol.* 231, 1173–1177.
- Okayama, H., Ueda, K., Hayaishi, O., 1980. NAD glycohydrolases from rat liver nuclei. *Methods Enzymol.* 66, 151–154.
- Richards, E.M., Rosenthal, R.E., Kristian, T., Fiskum, G., 2006. Postischemic hyperoxia reduces hippocampal pyruvate dehydrogenase activity. *Free Radic. Biol. Med.* 40, 1960–1970.
- Ridenour, T.R., Warner, D.S., Todd, M.M., McAllister, A.C., 1992. Mild hypothermia reduces infarct size resulting from temporary but not permanent focal ischemia in rats. *Stroke* 23, 733–738.
- Schaper, J., Schaper, W., 1983. Reperfusion of ischemic myocardium: ultrastructural and histochemical aspects. *J. Am. Coll. Cardiol.* 1, 1037–1046.
- Snell, C.R., Snell, P.H., Richards, C.D., 1984. Degradation of NAD by synaptosomes and its inhibition by nicotinamide mononucleotide: implications for the role of NAD as a synaptic modulator. *J. Neurochem.* 43, 1610–1615.
- Valero, E., Garcia-Carmona, F., 1996. Optimizing enzymatic cycling assays: spectrophotometric determination of low levels of pyruvate and L-lactate. *Anal. Biochem.* 239, 47–52.
- Valero, E., Varon, R., Garcia-Carmona, F., 1995. Kinetic study of an enzymic cycling system coupled to an enzymic step: determination of alkaline phosphatase activity. *Biochem. J.* 309, 181–185.
- Xia, W., Wang, Z., Wang, Q., Han, J., Zhao, C., Hong, Y., Zeng, L., Tang, L., Ying, W., 2009. Roles of NAD(+)/NADH and NADP(+)/NADPH in cell death. *Curr. Pharm. Des.* 15, 12–19.
- Ying, W., 2006. NAD⁺ and NADH in cellular functions and cell death. *Front. Biosci.* 11, 3129–3148.
- Ying, W., 2007. NAD⁺ and NADH in brain functions, brain diseases and brain aging. *Front. Biosci.* 12, 1863–1888.
- Ying, W., 2008a. NAD⁺ and NADH in ischemic brain injury. *Front. Biosci.* 13, 1141–1151.
- Ying, W., 2008b. NAD⁺/NADH and NADP⁺/NADPH in cellular functions and cell death: regulation and biological consequences. *Antioxid. Redox Signal.* 10, 179–206.
- Ying, W., Wei, G., Wang, D., Wang, Q., Tang, X., Shi, J., Zhang, P., Lu, H., 2007. Intranasal administration with NAD⁺ profoundly decreases brain injury in a rat model of transient focal ischemia. *Front. Biosci.* 12, 2728–2734.